



Magnetic navigation system for the precise helical and translational motions of a microrobot in human blood vessels

S. M. Jeon, G. H. Jang, H. C. Choi, S. H. Park, and J. O. Park

Citation: *J. Appl. Phys.* **111**, 07E702 (2012); doi: 10.1063/1.3671411

View online: <http://dx.doi.org/10.1063/1.3671411>

View Table of Contents: <http://jap.aip.org/resource/1/JAPIAU/v111/i7>

Published by the [American Institute of Physics](#).

Related Articles

Robotic reconnaissance platform. I. Spectroscopic instruments with rangefinders

Rev. Sci. Instrum. **82**, 113107 (2011)

Actuation of a robotic fish caudal fin for low reaction torque

Rev. Sci. Instrum. **82**, 075114 (2011)

Precise manipulation of a microrobot in the pulsatile flow of human blood vessels using magnetic navigation system

J. Appl. Phys. **109**, 07B316 (2011)

A tuning fork based wide range mechanical characterization tool with nanorobotic manipulators inside a scanning electron microscope

Rev. Sci. Instrum. **82**, 035116 (2011)

Dynamical network interactions in distributed control of robots

Chaos **16**, 015116 (2006)

Additional information on *J. Appl. Phys.*

Journal Homepage: <http://jap.aip.org/>

Journal Information: http://jap.aip.org/about/about_the_journal

Top downloads: http://jap.aip.org/features/most_downloaded

Information for Authors: <http://jap.aip.org/authors>

ADVERTISEMENT

LakeShore Model 8404 developed with **TOYO Corporation**
NEW AC/DC Hall Effect System Measure mobilities down to 0.001 cm²/V s

Magnetic navigation system for the precise helical and translational motions of a microrobot in human blood vessels

S. M. Jeon,¹ G. H. Jang,^{1,a)} H. C. Choi,² S. H. Park,² and J. O. Park²

¹PREM, Department of Mechanical Engineering, Hanyang University, Seoul 133-791, Korea

²Department of Mechanical Engineering, Chonnam National University, Gwangju, 500-757, Korea

(Presented 3 November 2011; received 20 September 2011; accepted 17 October 2011; published online 7 February 2012)

Different magnetic navigation systems (MNSs) have been investigated for the wireless manipulation of microrobots in human blood vessels. Here we propose a MNS and methodology for generation of both the precise helical and translational motions of a microrobot to improve its maneuverability in complex human blood vessel. We then present experiments demonstrating the helical and translational motions of a spiral-type microrobot to verify the proposed MNS. © 2012 American Institute of Physics. [doi:10.1063/1.3671411]

I. INTRODUCTION

Microrobots manipulated by a magnetic navigation system (MNS) in human blood vessels have been widely investigated for various medical purposes.¹⁻⁶ Since the principle of manipulation is based on the external magnetic field, the size and complexity of the microrobot can be effectively minimized so that it can navigate through the resistive environment of human blood vessels.¹⁻⁶

Several researchers have investigated MNSs to separately generate the helical or translational motions of a microrobot.¹⁻⁶ Zhang *et al.* showed that the rotating magnetic field generated by three pairs of circular coils can propel a spiral-type microrobot helically in a fluid,³ while Hyunchul *et al.* showed that the magnetic gradient generated from a rotatory MNS can axially translate a cylindrical microrobot on a surface.⁴ However, the helical and translational motions required for a microrobot have not been generated with one MNS due to the magnetic and structural restrictions of conventional MNSs.¹⁻⁶ Combination of helical and translational motion capabilities would greatly improve the maneuverability of a microrobot in complex human blood vessels.

Here we propose a novel type of MNS to achieve both helical and translational motions of a microrobot within one compact structure (Fig. 1). The MNS can be divided into Parts I and II, according to the type of magnetic field generation. Part I [Fig. 1(a)] is composed of one Helmholtz coil (HC) and two uniform saddle coils (USCs) capable of generating the rotating magnetic field, while Part II [Fig. 1(b)] is composed of one Maxwell coil (MC) and one gradient saddle coil (GSC) to generate the magnetic gradient.² Part II is inserted into Part I. In this paper, we calculate the input voltages of Part I to generate a precise rotating magnetic field by considering the frequency effect on the MNS. We also calculate the current relationship of the MC and GSC to translate the microrobot on a three-dimensional surface. Finally, we conduct several experiments to verify the efficacy of the proposed MNS.

II. GENERATION OF HELICAL AND TRANSLATIONAL MOTIONS OF A MICROBOT

The magnetic torque and force applied to a microrobot in a MNS can be expressed by the following equations:²

$$\vec{T} = \mu_0 V \vec{M} \times \vec{H}, \quad (1)$$

$$\vec{F} = \mu_0 V (\vec{M} \cdot \nabla) \vec{H}, \quad (2)$$

where μ_0 , V , \vec{M} , and \vec{H} are the magnetic permeability of free space, the volume, the magnetization of a microrobot, and the external magnetic field intensity, respectively. From Eqs. (1) and (2), a MNS can rotate or translate a microrobot independently.² The magnetic field near the center of the proposed MNS can be expressed as follows:²

$$\begin{aligned} \vec{H}_{MNS} = & [d_h + (g_g + g_m)x \quad d_{uy} + (-2.4398g_g - 0.5g_m)y \quad d_{uz} \\ & + (1.4398g_g - 0.5g_m)z]^T, \\ d_h = & (4/5)^{3/2} i_h / r_h, \quad d_{uy} = 0.6004 i_{uy} / r_{uy}, \\ d_{uz} = & 0.6004 i_{uz} / r_{uz}, \\ g_m = & (16/3)(3/7)^{5/2} i_m / r_m^2, \quad g_g = 0.3286 i_g / r_g^2, \end{aligned} \quad (3)$$

where i_k and r_k are the current and radius of the k th coil, and the subscripts h , m , g , uy , and uz represent the HC, MC, GSC, y and z -directional USCs, respectively. The axial unit vector \vec{N} and the magnetization angle δ from \vec{N} of a general

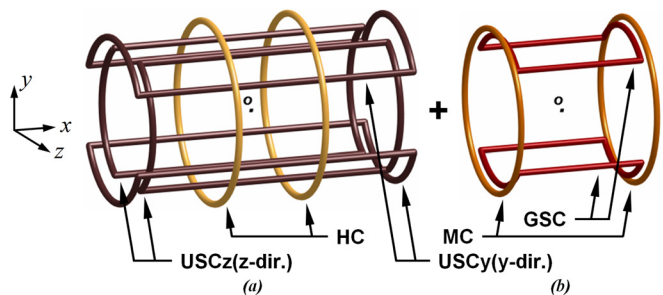


FIG. 1. (Color online) The proposed MNS divided into (a) Part I and (b) Part II.

^{a)} Author to whom correspondence should be addressed.

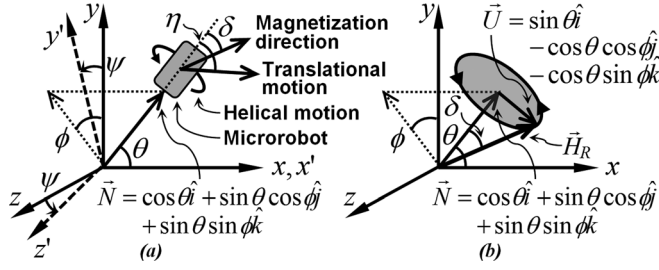


FIG. 2. (a) The microrobot in three-dimensional space. (b) Rotating magnetic field along \vec{N} .

spiral-type microrobot in three-dimensional space can be defined as shown in Fig. 2(a). To helically propel the microrobot along \vec{N} , the required rotating magnetic field shown in Fig. 2(b) can be expressed as follows:

$$\vec{H}_R(t) = H_0(\cos \delta \vec{N} + \sin \delta \cos \omega t \vec{U} + \sin \delta \sin \omega t \vec{N} \times \vec{U}), \quad (4)$$

where H_0 , ω , and \vec{U} are the magnitude and angular velocity of the rotating magnetic field, and a unit vector from \vec{N} toward a point on the circle, respectively. Equation (4) can also be used to align the microrobot when ω equals zero. Since the coils in Part I are geometrically symmetric and the currents in each pair of the coils flow in the same direction, the electromagnetic coupling effect of each set of HC and USCs does not exist,² and the frequency response of the HC and USCs can thus be independently calculated. Since coils are generally wound by hundreds of turns of wire, the resistances, inductances, and capacitances of the HC and USCs may vary with a change in frequency because of the skin and proximity effect.⁷ Thus, the frequency response of the HC and USCs can be expressed as follows:

$$i_k(j\omega) = (R_k(\omega) + j\omega L_k(\omega) + 1/(j\omega C_k(\omega)))^{-1} e_k(j\omega), \quad (5)$$

where L_k , R_k , C_k , and e_k are the inductance, resistance, capacitance, and the input voltage of the k th coil, respectively,

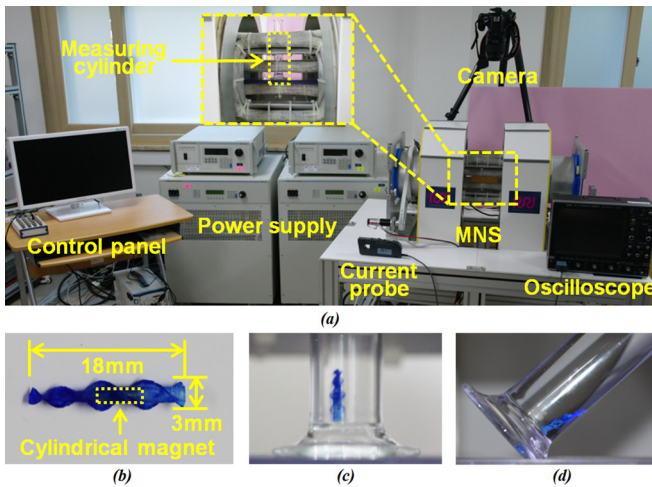


FIG. 3. (Color online) (a) Experimental setup for the proposed MNS. (b) Spiral-type microrobot. (c) Helical motion of the microrobot when $\theta = 90^\circ$ and $\phi = 0^\circ$, and (d) helical motion of the microrobot when $\theta = 45^\circ$ and $\phi = 0^\circ$.

TABLE I. Major specifications of the proposed MNS.

Coil	Radius (mm)	Wire diameter (mm)	Width (mm)	Height (mm)	Coil turns
MC	195	1.6	80	40	1123
HC	195	1.5	35	40	556
GSC	140	1.0	24	24	419
USCy	140	1.0	24	24	419
USCz	67	1.0	24	24	419

and the subscript k can be replaced by h , uy , and uz . Therefore, the proposed MNS can control the helical motion of the microrobot precisely by utilizing Eqs. (3), (4), and (5).

The proposed MNS is also capable of translating the microrobot parallel to the axial direction. When the magnetization of the microrobot is aligned by the HC and USCs on the xy' -plane [Fig. 2(a)], the conditions whereby the microrobot can be translated along the angle of η from \vec{N} can be expressed as follows:⁴

$$F_{y'} = mg \cos \psi + F_x \tan(\theta + \eta), \quad (6)$$

where m , g , ψ , θ , $F_{y'}$, and F_x are the mass of the microrobot, the gravitational acceleration, the rotating angle of the xy' -plane from the xy -plane, the angle between \vec{N} and the x -axis, and the component of the magnetic force along the y' -axis and the x -axis, respectively. From Eqs. (2), (3), and (6), the relationship of the currents between the MC and the GSC for the translational motion of the microrobot can be derived, provided that the MC is rotatable along the x -axis according to the angle ψ .⁴

III. RESULTS AND DISCUSSION

In this study, we constructed an experimental setup to verify the proposed MNS to achieve helical and translational motion of a microrobot (Fig. 3; Table I). The resistances, inductances, and capacitances of the HC and USCs were measured using a LCR-meter at different frequencies (Fig. 4). We prototyped a spiral-type microrobot [Fig. 3(b)], with a transversely magnetized cylindrical neodymium magnet ($\delta = 90^\circ$) inserted into it. The diameter, length, and

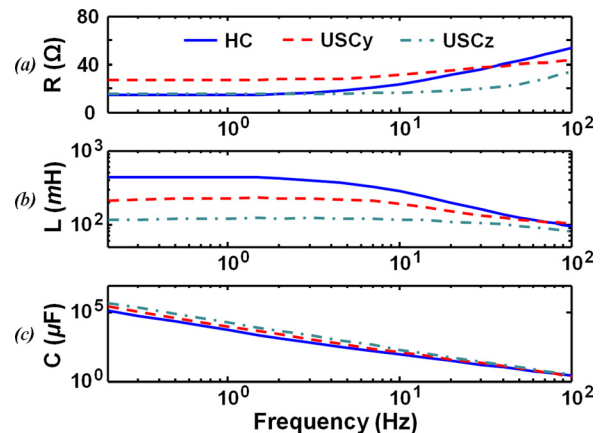


FIG. 4. (Color online) Measured (a) resistances, (b) inductances, and (c) capacitances of the HC and USCs at frequencies ranging from 0 to 100 Hz.

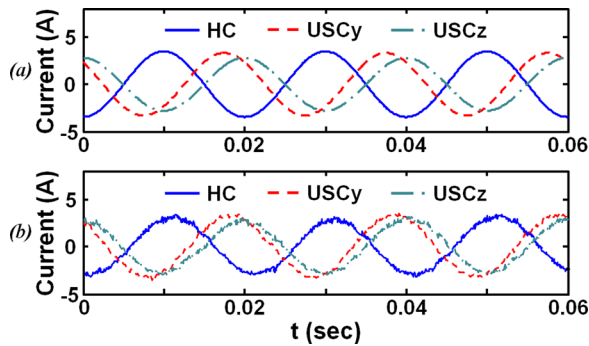


FIG. 5. (Color online) (a) Calculated and (b) measured currents of the HC and USCs for the helical motion of the microrobot when $\theta = 45^\circ$, $\phi = 0^\circ$, and $f = 50$ Hz.

magnetization of the magnet are 1 mm, 5 mm, and 955 000 A/m, respectively. In a measuring cylinder filled with water [Figs. 3(c) and 3(d)], the microrobot showed sufficiently fine helical motions in the range of the rotating frequency $f = 0 - 100$ Hz for input voltages calculated using Eqs. (3), (4), (5), and Fig. 4 when $\theta = 90^\circ$, $\phi = 0^\circ$ and $\theta = 45^\circ$, $\phi = 0^\circ$, respectively. The resultant currents in the HC and USCs for $\theta = 45^\circ$, $\phi = 0^\circ$, and $f = 50$ Hz were measured

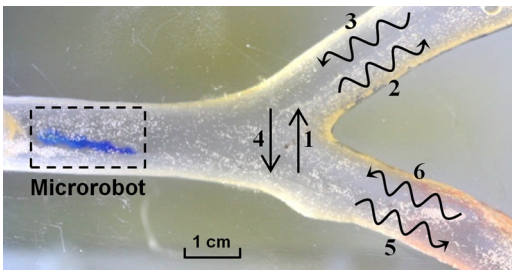


FIG. 6. (Color online) The translational motions (Steps 1 and 4) and the backward and forward helical motions (Steps 2, 3, 5, and 6) of the microrobot in a blood vessel phantom.

with a current probe and were found to match well with the calculated values (Fig. 5). Finally, we demonstrated the sequential helical and translational motions of the microrobot in a horizontally placed blood vessel phantom filled with water (Fig. 6). In Fig. 6, Steps 1 and 4 are the translational motions that allow transverse movement of the microrobot when choosing which branch to enter, and Steps 2, 3, 5, and 6 are the forward and backward helical motions capable of axially propelling or drilling the clogged area in the blood vessel.

IV. CONCLUSIONS

In this paper, we proposed one MNS capable of realizing both helical and translational microrobot motions. We introduced methods to precisely generate these motions and experimentally verified the efficacy of the proposed MNS. This research could be extended to the precise and effective manipulation of a microrobot in several organs of the human body such as the central nervous system, the urinary system, the eye, and others.

ACKNOWLEDGMENTS

This research was supported by the Strategy Technology Development Program (No. 10030037) of the Korean Ministry of Knowledge Economy.

- ¹B. J. Nelson, I. K. Kaliakatsos, and J. J. Abbott, *Annu. Rev. Biomed. Eng.* **12**, 55 (2010).
- ²S. Jeon, G. Jang, H. Choi, and S. Park, *IEEE Trans. Magn.* **46**(6), 1943 (2010).
- ³L. Zhang, K. E. Peyer, and B. J. Nelson, *Lab on a Chip* **10**(17), 2177 (2010).
- ⁴H. Choi, K. Cha, J. Choi, S. Jeong, S. Jeon, G. Jang, J. Park, and S. Park, *Sensors and Actuators A* **163**, 410 (2010).
- ⁵S. Jeon, G. Jang, J. Choi, S. Park, and J. Park, *J. Appl. Phys.* **109**, 07B316 (2011).
- ⁶S. Jeon, G. Jang, H. Choi, S. Park, and J. Park, *IEEE Trans. Magn.* **47**(10), 2403 (2011).
- ⁷S. Mei and Y. Ismail, *IEEE Trans. VLSI Sys.* **12**(4), 437 (2004).